Stabilization of Z-DNA by Demethylation of Thymine Bases: 1.3-Å Single-Crystal Structure of d(m^5CGUAm^5CG)†

Guangwen Zhou and Pui S. Ho*

Department of Biochemistry and Biophysics, Oregon State University, Corvallis, Oregon 97331

Received December 18, 1989; Revised Manuscript Received March 26, 1990

ABSTRACT: Methylation of cytosine bases at the C5 position has been known to stabilize Z-DNA. We had previously predicted from calculations of solvent-accessible surfaces that the methyl group at the same position of thymine has a destabilizing effect on Z-DNA. In the current studies, the sequence d(m^5CGUAm^5CG) has been crystallized and its structure solved as Z-DNA to 1.3-Å resolution. A well-defined octahedral hexaaquomagnesium complex was observed to bridge the O4 oxygens of the adjacent uridine bases at the major groove surface, and four well-structured water molecules were found in the minor groove crevice at the d(UA) dinucleotide. These solvent interactions were not observed in the previously published Z-DNA structure of the analogous d(m^5CGTAm^5CG) sequence. A comparison of the thymine and uridine structures supports our prediction that demethylation of thymine bases helps to stabilize Z-DNA. A comparison of this d(UA)-containing Z-DNA structure with the analogous d(TA) structure shows that access of the O4 position is hindered by the C5 methyl of thymine due to steric and hydrophobic inhibition. In the absence of the methyl group, a magnesium–water complex binds to and slightly affects the structure of the Z-DNA major groove surface. This perturbation of the solvent structure at the major groove surface is translated into a much larger 1.41-Å widening of the minor groove crevice, thereby allowing the specific binding of two water molecules at well-defined sites of each internal d(UA) base pair. Possible mechanisms by which modifications at the major groove surface of Z-DNA can affect the solvent properties of the minor groove crevice are discussed.

Left-handed Z-DNA has been shown to be stabilized by many factors, including dehydrating conditions such as high salt and alcohol concentrations, specific interactions of the DNA bases with metal complexes, and modification of bases such as methylation or bromination of cytosine at the C5 position [reviewed by Rich et al. (1984) and Jovin et al. (1987)]. The propensity of DNA to adopt the Z-conformation is also dependent on its base sequence, with alternating pyrimidine and purine sequences being more adaptable than sequences that do not follow this alternation rule (Wang et al., 1981; Drew & Dickerson, 1981; Jovin et al., 1983). Within the series of dinucleotide sequences that do follow the alternation rule, the order d(CG) > d(CA)-d(TG) > d(TA) has been observed in terms of the stability of dinucleotides as Z-DNA (Jovin et al., 1983). The relative inability of d(TA) dinucleotides to adopt the Z-conformation, however, has not been adequately described from enthalpic calculations of base stacking, hydrogen bonding, steric interactions, and electrostatic interactions (Kollman et al., 1982). We recently showed that d(TA) does not readily form Z-DNA largely because the C5 methyl group renders the major groove surface more hydrophobic in the Z versus the B-conformation (Kagawa et al., 1989). This contrasts the effect of methylation of cytosine. The effect of methylation on Z-DNA stability, therefore, is also sequence dependent.

Methylation of cytosines at the C5 position has been shown to stabilize Z-DNA in solution (Behe & Felsenfeld, 1981). The cytosine methyl group in the crystal structure of d(m^5CG)$_3$ sits in a pocket on the major groove surface of Z-DNA, thereby effectively decreasing the exposure of the major groove surface to solvent (Fujii et al., 1982). When we quantitated this effect on the major groove surface, this C5 pocket was observed to be lined primarily by hydrophobic atoms (Ho et al., 1988). The increased hydrophobicity of the major groove surface that one would expect from methylation at this site is thus entirely negated by the decreased exposure of hydrophobic surfaces lining the C5 pocket. Using this same analysis, we found that the C5 pocket in d(TA) dinucleotides as Z-DNA is more hydrophilic than that of d(m^5CG)$_3$ (Kagawa et al., 1989). The methyl group of d(TA) therefore decreases the exposure of hydrophilic groups to solvent while increasing the hydrophobic character of the major groove surface of Z-DNA. This has the effect of decreasing the stability of d(TA) as Z-DNA and was estimated to account for roughly half the difference in the thermodynamic stability of d(TA) versus d(CG) dinucleotides as Z-DNA. The other major difference between d(CG) and d(TA) dinucleotides in terms of the Z-DNA surface exposed to solvent lies in the minor groove crevice. The hydrophilic N2 amino group of the guanine base of d(CG) dinucleotides sits in the minor groove crevice of the Z–DNA structure. This amino group is not present on the adenine base of d(TA) dinucleotides. The surface of the minor groove crevice of d(TA) dinucleotides in the Z-conformation is thus less hydrophilic than that of d(CG), and this also contributes to the instability of d(TA) dinucleotides as Z-DNA.

From these considerations of hydration energies on the stability of DNA conformations, d(UA) dinucleotides were predicted to be more stable than d(TA) as Z-DNA (Kagawa et al., 1989). The hydrophilic groups at the major groove surface of d(UA) dinucleotides were shown to be more accessible to solvent than those of the d(TA) dinucleotides, while the hydrophobicity of the minor groove, to the first approximation, remained the same. Therefore, d(UA) dinucleotides were predicted to have the same propensity to adopt the Z-conformation as would d(CA)-d(TG). In this current study, we have crystallized the self-complementary sequence d-

† This work was supported by NIEHS Grant ES00210 and by the Office of Naval Research (Contract N00014-88-K-0388).

* To whom correspondence should be addressed.

0006-2960/90/0429-7229$02.50/0

Table I: Comparison of Crystallization Conditions and Unit-Cell Parameters of $d(m^5CG)_3$, $d(m^5CGUAm^5CG)$, and $d(m^5CGTAm^5CG)$[a]

	sequence		
	$d(m^5CG)_3$	$d(m^5CGUAm^5CG)$	$d(m^5CGTAm^5CG)$
initial crystallization concentrations			
hexamer (mM)	2	4	4
sodium cacodylate (pH 7.0) (mM)	30	28	30
magnesium chloride (mM)	4	15	15
spermine (mM)	0	0	7
precipitant	2% 2-MPD	8.5% 2-MPD	8% 2-MPD
reservoir	10% 2-MPD	30% 2-MPD	50% 2-MPD
CS at equilibrium (M)	0.23	0.31	0.56
unit-cell dimensions of crystal			
a (Å)	17.76	17.82	17.91
b (Å)	30.57	30.44	30.43
c (Å)	45.42	44.52	44.96
space group	$P2_12_12_1$	$P2_12_12_1$	$P2_12_12_1$
ref	Fujii et al., 1982	this work	Wang et al., 1984

[a] Listed are the initial crystallization conditions, the equilibrium cationic strengths (CS) calculated from the sodium and magnesium salt concentrations at equilibrium, and the unit-cell parameters of each crystal. 2-MPD is 2-methyl-2,4-dimethylpentanediol. CS is the cation strength at equilibrium for the conditions at which diffraction-quality Z-DNA crystals of each hexamer were obtained (see text).

(m^5CGUAm^5CG) and found that it crystallized as Z-DNA under conditions of significantly lower salt concentrations when compared to its thymine analogue $d(m^5CGTAm^5CG)$ (Wang et al., 1984). Furthermore, the 1.3 Å resolution structure of the $d(m^5CGUAm^5CG)$ crystal revealed that specific interactions of cation complexes at the major groove surface and water molecules in the minor groove crevice are present for d(UA) structure but were absent from the reported structure of d(TA) dinucleotides in Z-DNA (Wang et al., 1984). The results from this present study support our assertion that the C5 methyl of thymine plays a major role in the instability of d(TA) as Z-DNA. In addition, we propose possible mechanisms by which this methyl at the major groove surface alters the structure and solvent properties of the minor groove crevice of Z-DNA.

Experimental Procedures

The hexanucleotide $d(m^5CGUAm^5CG)$ was synthesized on an Applied Biosystems DNA synthesizer. The purity of the original oligonucleotide was estimated to be better than 94% from the coupling efficiencies. All blocking reagents and precursors were removed by Sephadex G-10 column chromatography. The hexanucleotide was crystallized at room temperature according to the vapor diffusion method, with 30% 2-methyl-2,4-pentanediol (2-MPD) as the precipitating agent. The initial crystallization solution contained 4.0 mM oligonucleotide, 28 mM sodium cacodylate buffer at pH 7.0, 15 mM magnesium chloride, and 8.5% 2-MPD. Yellowish crystals that were not suitable for X-ray diffraction studies formed overnight under these conditions. These crystals were collected, washed with several volumes of cold distilled, deionized water, and redissolved in water. In the next round of crystallization using the recrystallized oligonucleotide, large nearly colorless crystals were obtained after 3 days under conditions identical with those of the original crystallization step.

X-ray diffraction data were collected at room temperature from a 0.3 mm × 0.5 mm × 0.5 mm crystal on a Rigoku diffractometer. The crystal has a space group of $P2_12_12_1$, typical of the lattice of previous Z-DNA hexamer crystals, with unit-cell dimensions of a = 17.82 Å, b = 30.44 Å, and c = 44.52 Å. This crystal diffracted to better than 1.3-Å resolution. The structure of this crystal was refined with the Konnert–Hendrickson restrained refinement method (Hendrickson & Konnert, 1979). The initial model for refining the structure was generated from the 1.2 Å resolution Z-DNA structure of $d(m^5CGTAm^5CG)$ (Wang et al., 1984) in which the methyl groups of the thymine bases were removed from the C5 positions. Of the 3869 reflections collected, the intensities of 2870 reflections were greater than 2σ and were included in the structure refinement. The structure was refined to better than 1.3-Å resolution, with a final R factor of 20.8%. In the course of refinement, 62 well-defined water molecules and 2 unique magnesium–water complexes were located in the asymmetric unit.

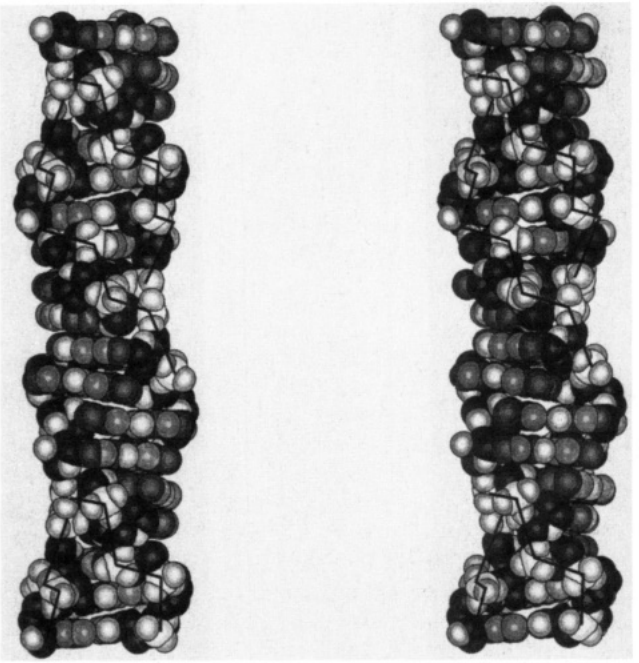

FIGURE 1: Stereo diagram of the $d(m^5CGUAm^5CG)$ van der Waals surface. Shown are three hexamers stacked end-to-end along the crystallographic *c* axis. Each hexamer is related by 2-fold screw symmetry along the helical axis to generate a continuous one and one-half turn of Z-DNA. From dark to light, the atoms are coded as ribose carbons, base carbons, nitrogens, oxygens, and phosphorus.

Results

Structure of $d(m^5CGUAm^5CG)$. The self-complementary hexamer sequence $d(m^5CGUAm^5CG)$ crystallizes as Z-DNA in a lattice that is isomorphous with those of previous hexanucleotide Z-DNA crystals (see Table I). The stereo diagram in Figure 1 shows the van der Waals surface of three $d(m^5CGUAm^5CG)$ hexamers stacked end-to-end along the crystallographic *c* axis. The phosphorus atoms of the backbone are connected to show the zigzag pattern characteristic of

Z-DNA. As with all previous Z-DNA structures, the two strands of the hexamer duplex from antiparallel strands with Watson–Crick base pairs. The purine bases are in the syn conformation, and the pyrimidine bases are in the anti conformation.

Crystallization of d(m^{5}CGUAm^{5}CG). To obtain a measure of the ability of d(UA) dinucleotides, relative to other alternating pyrimidine–purine sequences, to adopt the Z-conformation, we compared the equilibrium salt concentrations present in the solutions that provide diffraction-quality crystals of Z-DNA for self-complementary hexamer DNAs with the general sequence d(m^{5}CGPyPum^{5}CG). The nucleotide Py in this sequence represents a pyrimidine base, d(m^{5}C), d(T), or d(U), and Pu represents a purine base, d(G) or d(A). The premise behind this comparison is that a critical concentration of hexamers in the Z-conformation must be present in solution prior to crystallization of that sequence as Z-DNA. Z-DNA has been shown to be stabilized by salt, and the concentration of salt required to stabilize Z-DNA is dependent on the relative ability of sequences to adopt the Z-conformation. A comparison of the equilibrium concentrations of salt in the crystallization setups, therefore, provides a measure of how changing the internal PyPu dinucleotide affects the ability of the general sequence to adopt the Z-conformation.

In a previous study, the concentration of cations required to obtain diffraction-quality crystals for four well-studied alternating pyrimidine and purine hexamer sequences, d-(m^{5}CG)$_3$, d(m^{5}CGTAm^{5}CG), d(CG)$_3$, and d(CACGTG), as Z-DNA was shown to be dependent on the relative abilities of these sequences to form Z-DNA. We found it useful to define the quantity of cationic strength to facilitate the analysis of the equilibrium cation properties when comparing the crystallization conditions of hexamer sequences as Z-DNA. The stability of Z-DNA is dependent on both the concentration and the charge of the cations in solution. The anions present in the crystallization conditions do not appear to play as significant a role in Z-DNA stability as do cations. Cationic strength (CS), therefore, was defined as CS = $\sum Z_i^2 C_i$, where Z_i is the charge and C_i is the concentration of the ith cation (Kagawa et al., 1989). When this was converted to the quantity log CS at equilibrium, we observed a linear relationship between the crystallization conditions and the free energy difference between B- and Z-DNA for the four hexamer sequences. The crystallization conditions mirror the difference in salt concentrations required to induce Z-DNA formation in polymeric DNA and generally follow the expected hierarchy of d(m^{5}CG) > d(CG) > d(CA)-d(TG) > d(TA) in the ability of dinucleotides to adopt the Z-conformation. The equilibrium cationic strength required to form diffraction-quality Z-DNA crystals therefore appears to be a useful measure for the ability of a hexamer sequence to form Z-DNA.

The initial and equilibrium conditions for crystallizing the hexamer sequences d(m^{5}CG)$_3$, d(m^{5}CGUAm^{5}CG), and d-(m^{5}CGTAm^{5}CG) as Z-DNA are compared in Table I. The equilibrium salt concentrations required to crystallize the hexamer sequence d(m^{5}CGUAm^{5}CG) as Z-DNA were significantly lower than those for d(m^{5}CGTAm^{5}CG) (Wang et al., 1984). Although the initial salt concentrations for d-(m^{5}CGUAm^{5}CG) and d(m^{5}CGTAm^{5}CG) were similar, the final concentrations at equilibrium were quite different because of the higher precipitant concentration used to drive the crystallization of d(m^{5}CGTAm^{5}CG). The polycation spermine was not found in the crystal of d(m^{5}CGTAm^{5}CG) even though it was present in the crystallization conditions (Wang et al., 1984). Only the sodium and magnesium concentrations were thus used in calculating cationic strength for crystallizing d(m^{5}CGTAm^{5}CG). We have confirmed that indeed d-(m^{5}CGTAm^{5}CG) can be crystallized under this cationic strength in the absence of spermine.

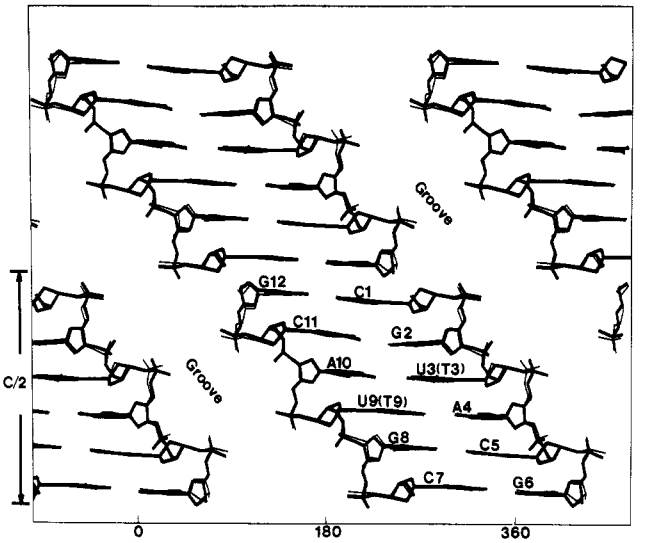

FIGURE 2: Polar projection comparing the structures of d-(m^{5}CGUAm^{5}CG) and d(m^{5}CGTAm^{5}CG). The d(m^{5}CGUAm^{5}CG) structure is shown as thick bonds and the d(m^{5}CGTAm^{5}CG) structure shown as thin bonds. The polar projection was generated as described in the text. The x axis is the angle of view around the helical axis, and the y axis is the helical axis ($c/2$ is one-half the length of the crystallographic c axis). The minor groove crevice is labeled.

A comparison of the cationic strengths of three Z-DNA hexamers shows that the sequence d(m^{5}CGUAm^{5}CG) required a 1.64 times lower concentration of total cations to crystallize as Z-DNA as compared with d(m^{5}CGTAm^{5}CG) and 1.57 times higher than that required for d(m^{5}CG)$_3$. These differences in cation strength are in the magnitude of 100–200 mM cation concentrations and therefore represent significant differences in crystallization conditions. This supports our previous prediction that the propensity of d(UA) dinucleotides to adopt the Z-conformation is greater than that of d(TA) but lower than that of d(m^{5}CG) dinucleotides. We assume in this comparison that a critical concentration of DNA must be in the Z-conformation at equilibrium before it will actually crystallize as Z-DNA.

Comparison of the d(m^{5}CGUAm^{5}CG) DNA Structure with That of d(m^{5}CGTAm^{5}CG). Overall, the Z-DNA structures of d(m^{5}CGUAm^{5}CG), which we report in this study, and d(m^{5}CGTAm^{5}CG), as previously reported (Wang et al., 1984), are very similar. These structures are compared in Figure 2 as superimposed polar projections of the Z-DNA helices. A polar projection is generated by projecting the atomic coordinates of the DNA, the helix axis being used as the origin of the projection, onto a cylindrical surface wrapped around the helix. When the surface is unwrapped along the helical axis, the resulting projection allows us to view all angles of the DNA at once, including the major groove surface and the minor groove crevice. The structure of d(m^{5}CGUAm^{5}CG) is shown as thick bonds while that of d(m^{5}CGTAm^{5}CG) is shown as thin bonds. The nucleotides are numbered 1–6 for the 5′ to 3′ direction along one strand and 7–12 along the opposite strand. In general, the projected structures of d-(m^{5}CGUAm^{5}CG) and d(m^{5}CGTAm^{5}CG) nearly completely overlap, consistent with the low overall root-mean-square (RMS) deviation of 0.34 Å calculated between the two structures. The RMS deviation base to base is 0.05–0.08 Å, ribose to ribose is 0.07–0.18 Å, and nucleoside to nucleoside

Table II: Comparison of the Distances Separating Corresponding Atoms at the Major Groove Surface and at the Minor Groove Crevice of d(UA) and d(TA) Dinucleotides as Z-DNA[a]

atom names	atomic distances (Å)		
	d(TA)	d(UA)	d(UA) − d(TA)
Py3 O4---Py9 O4	3.83	3.84	0.01
Py3 O2---Py9 O2	3.68	3.55	−0.13
Py3 C3′---Py9 C3′	10.69	10.64	−0.05
Py3 O3′---Py9 O3′	9.69	10.04	0.35
A4 P---A10 P	11.48	12.32	0.84
A4 O1P---A10 O2P	9.71	11.12	1.41

[a] The nomenclature for the atom names is as follows. The residue name precedes the residue number. This is followed by the atom name and number. The residue Py is a pyrimidine nucleotide, either thymidine or deoxyuridine. O4 atoms represent the oxygens at the O4 position of the pyrimidine bases, C3′ and O3′ are the carbons and oxygens, respectively, at the 3-position of the ribose, P is the phosphorus of the phosphodiester, and O1P and O2P are two different oxygens of the phosphate group. The atomic distances are listed as distances between the opposing atoms on either side of the Z-DNA helix within the d(TA) dinucleotide and within the d(UA) dinucleotide. The d(UA) − d(TA) distances are differences between the d(UA) and d(TA) dinucleotide distances.

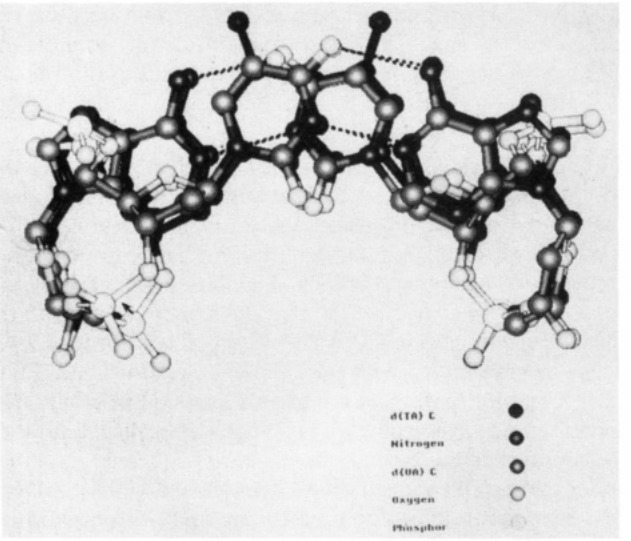

FIGURE 3: Comparison of the base-pair stacking of d(UA) dinucleotides and d(TA) dinucleotides along the helical axis of the Z-DNA. The structure of the d(UA) dinucleotide is shown stacked above the analogous d(TA) dinucleotide. The coding of the atoms as different intensities of gray is shown in the figure key. The arrow indicates rotation of a phosphate diester out and away from the minor groove crevice when going from d(TA) to d(UA) dinucleotides in Z-DNA. The differences in the distances separating atoms in the major groove surface and minor groove crevice are compared for the d(TA) and d(UA) dinucleotides as Z-DNA in Table II.

is 0.09–0.16 Å between the two structures. The largest deviations between groups, the methyl of the thymine bases being ignored, comes from the inversion of the sugar pucker of guanine G12 of d(m^{5}CGUAm^{5}CG) relative to d(m^{5}CGTAm^{5}CG). The ribose at the G12 nucleotide of d(m^{5}CGUAm^{5}CG) assumes a 3′-endo pucker while that of d(m^{5}CGTAm^{5}CG) is 2′-endo. This effectively rotates the phosphodiester linkage between C11 and G12 toward the minor groove crevice in d(m^{5}CGUAm^{5}CG). The sugar puckers of all other purine nucleotides are identical for both structures, with the G6 nucleotide adopting the C2′-endo conformation and all others in the C3′-endo conformation. The puckers of the ribose in all the pyrimidine nucleotides of both sequences are C2′-endo.

A more subtle, but perhaps more important, difference between the Z-DNA structures of d(m^{5}CGTAm^{5}CG) (Wang et al., 1984) and d(m^{5}CGUAm^{5}CG) that is not obvious from comparisons of their overall structures is seen when the conformations at the internal d(TA) and d(UA) dinucleotides are compared. A comparison of the base-pair stackings of d(TA) and d(UA) along the helical axis of Z-DNA is shown in Figure 3. The distances separating corresponding atoms that define the major groove surface and the minor groove crevice of the d(UA) and d(TA) dinucleotides are compared Table II. The O4 oxygens of adjacent base pairs in the d(TA) dinucleotides are separated by 3.83 Å. The same distance for d(UA) is 3.84 Å, only a 0.01-Å difference between the positions of the pyrimidine bases at the major groove crevice. This is an overall small difference between the d(UA) and the d(TA) bases but, in actual fact, represents a 0.2-Å shift in the plane of the A4-U9 base pair relative to the U3-A10 base pair when compared to the analogous base pairs of the d(TA) dinucleotide. The d(UA) base pairs are rolled 3° toward each other along the helical axis relative to the d(TA) base pairs. This roll compensates for the shift in the base-pair plane and results in the small overall difference in distances observed between the O4 oxygens at the major groove surface of the two types of base pairs in Z-DNA.

In the minor groove, the adjacent base pairs of the d(TA) dinucleotide are separated by 3.68 Å for the O2 to O2 of the purine base, 10.69 Å for C3′ to C3′ of the ribose, 9.69 Å for O3′ to O3′ of the ribose, 11.48 Å for phosphorus to phosphorus atoms, and 9.71 Å for the closest approach of the bridging phosphate oxygens. These same distances are 3.55 Å for O2 to O2, 10.64 Å for C3′ to C3′, 10.04 Å for O3′ to O3′, 12.32 Å for P to P, and 11.12 Å for the closest approach of the bridging phosphate oxygens in the minor groove crevice of the d(UA) dinucleotide. Thus, the minor groove crevice for the adjacent d(UA) relative to the d(TA) base pairs narrows when going from the C3′ of the ribose sugars toward the purine bases and widens going from the O3′ of the ribose toward phosphodiester linkage. This makes the minor groove crevice of the d(UA) dinucleotide 1.41 Å wider at the outer edges and renders it more accessible to water molecules when compared to the d(TA) dinucleotide in Z-DNA. The major groove surface, meanwhile, remains essentially the same in both structures.

Comparison of the Solvent and Cation Structures around d(m^{5}CGUAm^{5}CG) and d(m^{5}CGTAm^{5}CG). In the course of refining the structure of d(m^{5}CGUAm^{5}CG) to 1.3 Å, 62 well-ordered water molecules were located, while 98 water molecules were reported for the Z-DNA structure of d(m^{5}CGTAm^{5}CG) at 1.2-Å resolution (Wang et al., 1984). The lower number of water molecules assigned in the d(m^{5}CGUAm^{5}CG) structure reflects the slightly lower resolution of the data obtained from this crystal and the more conservative assignments of solvent within the structure. The electron densities of the water molecules immediately surrounding the DNA base pairs in the d(m^{5}CGUAm^{5}CG) structure are shown in the six sections of the map in Figure 4. Hydrogen bonds are shown as dotted lines connecting the bonded pairs. The d(m^{5}CG) base pairs and the water molecules immediately surrounding them are shown in panels A, B, E, and F. We noted that there are two well-defined water molecules in the minor groove crevice of each d(m^{5}CG) base pair, consistent with what has been observed in the minor groove crevices of the d(CG) and d(m^{5}CG) base pairs in all high-resolution structures of Z-DNA studied so far (Jovin et al., 1987). In the case of the d(CG)$_3$ (Wang et al., 1979) and d(m^{5}CG)$_3$ (Fujii et al., 1982) structures, these waters form a continuous spine along the minor groove that is thought to be important for stabilizing Z-DNA in these sequences.

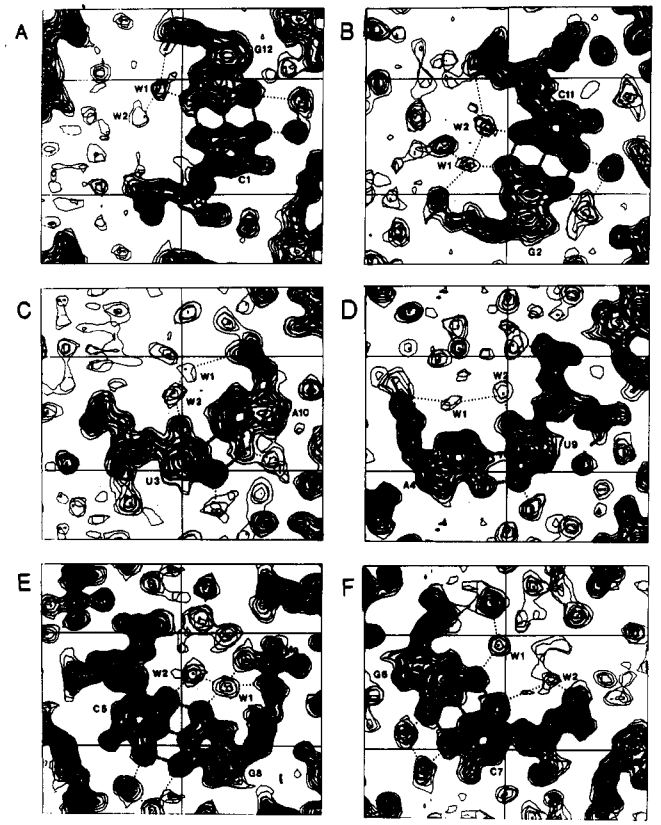

FIGURE 4: Sections from the electron density map at 1.3-Å resolution of d(m^{5}CGUAm^{5}CG). Panel A shows sections through C1-G12 base pairs, B shows G2-C11, C shows U3-A10, D shows A4-U9, E shows C5-G8, and F shows G6-C7. Each section is 3 Å thick. Hydrogen bonds are shown as dotted lines connecting the hydrogen-bond pairs. The electron densities associated with water molecules in the minor groove crevice are labeled as W1 and W2 for each base pair.

We also observed two well-defined water molecules in the minor groove crevice at each d(UA) base pair of the d(m^{5}CGUAm^{5}CG) structure (Figure 4C,D). These water molecules were not observed in the crevice of the d(TA) base pairs of the reported d(m^{5}CGTAm^{5}CG) (Wang et al., 1984) or d(CACGTG) (Coll et al., 1988) structures. This does not imply that waters do not reside in the Z-DNA crevice of d(TA) base pairs, only that they are either disordered or are poorly occupied within the groove. The increased width of the d(UA) minor groove crevice may help to define distinct water binding sites within the d(UA) crevice that are not accessible in the crevice of d(TA) base pairs. Alternatively, the binding of these waters may induce the widening of the d(UA) dinucleotide minor groove. Regardless of the explicit mechanism, it is clear that this spine of waters in the minor groove crevice of Z-DNA is interrupted by d(TA) base pairs but not by d(UA) base pairs. Thus, if indeed this spine of waters proves to be an essential element in the stability of the Z-conformation, d(UA) base pairs are less disruptive to, and therefore more stable as, Z-DNA than are d(TA) base pairs.

The other important solvent interaction in terms of Z-DNA stability is that of cations, and their aquo complexes, with the backbone and the bases. In the d(m^{5}CGUAm^{5}CG) structure, two crystallographically unique magnesium–water complexes were located within the asymmetric unit of the crystal. When we consider the symmetry of the crystal, four magnesium clusters would be located for each hexamer duplex. One magnesium cluster is directly coordinated to an oxygen of the phosphate linking nucleotide G8 with U9 (Figure 5A). Free water molecules in the minor groove crevice bridge this cluster to the phosphates that link nucleotides C7 to G8 and U9 to A10 of this same hexamer. On an adjacent hexamer, this magnesium cluster forms hydrogen bonds with the oxygens of the phosphate linking nucleotides A4 to C5 and C5 to G6. An analogous magnesium–water cluster was observed in the Z-DNA structure of d(m^{5}CGTAm^{5}CG) (Wang et al., 1984), suggesting that this cation complex is not directly affected by the C5 methyl group of the thymine bases.

A second crystallographically unique magnesium–water cluster in the d(m^{5}CGUAm^{5}CG) structure (Figure 5B) forms a hydrogen bond to an oxygen of the phosphate linking nucleotide U9 with A10. In addition, this complex forms hydrogen bonds with the O4 oxygens of the two adjacent uridine bases, thereby bridging the internal d(UA) dinucleotides, as shown in the sections through the electron density map of the

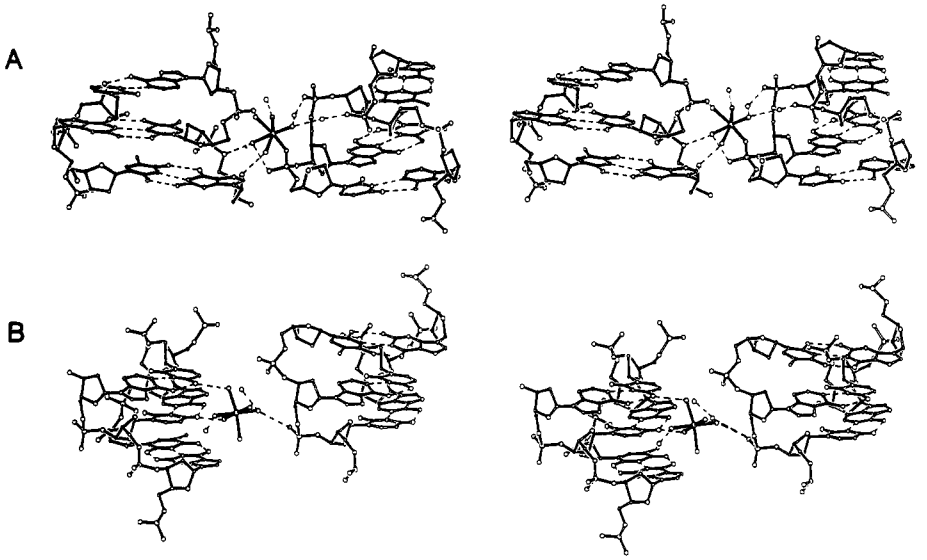

FIGURE 5: Stereo pair showing ball and stick models for interactions between the magnesium–water complexes and the DNA within the structure of d(m^{5}CGUAm^{5}CG). Hydrogen bonds are shown as dotted lines connecting the hydrogen-bonded pairs. (A) The pentaaquomagnesium complex is shown directly coordinated to the oxygen of the phosphate group linking nucleotides G8 with U9. The interactions of this magnesium complex with an adjacent d(m^{5}CGUAm^{5}CG) hexamer are shown along with bridging water molecules. (B) The hexaaquomagnesium complex is shown bridging nucleotides U3 and U9 of d(m^{5}CGUAm^{5}CG). The interactions of this magnesium complex with an adjacent d(m^{5}CGUAm^{5}CG) hexamer is also shown.

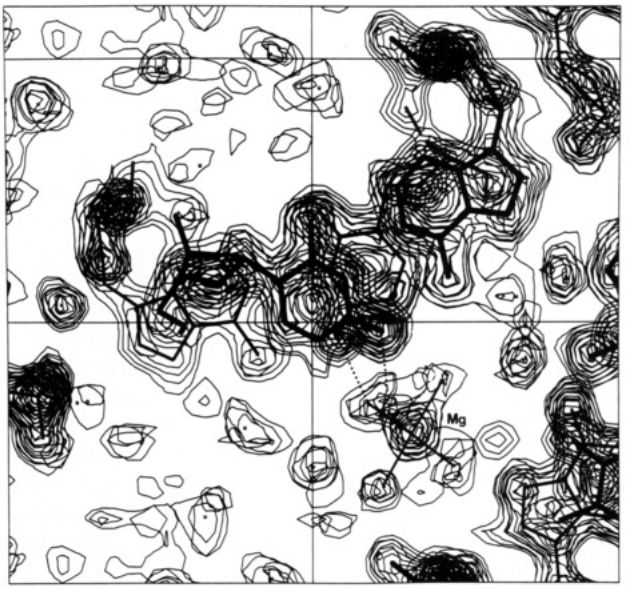

FIGURE 6: A 4 Å thick section through the electron density map of d(m^5CGUAm^5CG) showing the hexaaquomagnesium complex bridging the adjacent uridine bases of the internal d(UA) dinucleotides. Hydrogen bonds between the waters of the metal cluster with the O4 oxygens of the bases are shown as dotted lines.

two adjacent d(UA) base pairs (Figure 6). The adjacent uridine bases of the internal d(UA) dinucleotides are thus structurally linked at the major groove surface by the relatively rigid octahedral geometry of the magnesium cluster.

This structurally well-defined octahedral magnesium bridge was not observed in the Z-DNA structure of d(m^5CGTAm^5CG). A cluster of cations was previously observed at the major groove surface of d(m^5CGTAm^5CG). Within this cluster a single well-defined magnesium–water cluster was found bridging the N7 of guanine G8 and the O4 of thymine T9. The remainder of the cations within this cluster could not be definitely assigned to either magnesiums or sodiums because of the large distortions in their coordination geometries. The two cations at the major groove surface of the internal d(TA) dinucleotide are very distorted in terms of bond lengths and bond angles for the cation to water ligand bonds. These cations are most likely sodium ions with highly distorted coordination geometries, as opposed to the well-ordered magnesium complex at the d(UA) dinucleotides. Since the major groove surfaces of d(UA) and d(TA) are nearly identical in geometry, the disruption of these solvent interactions at the O4 oxygens must be due to the two hydrophobic methyl groups at the C5 positions of the thymine base and is consistent with the predictions from calculations of solvent-accessible surfaces of d(TA) and d(UA) dinucleotides in Z-DNA (Kagawa et al., 1989).

Figure 7 summarizes the solvent interactions around the internal d(UA) dinucleotide in the d(m^5CGUAm^5CG) structure. The octahedral magnesium–water cluster is shown bridging the O4 oxygens of the adjacent uridine bases, along with the water interactions within the minor groove crevice of the Z-DNA structure. These specific interactions of cation complexes at the major groove surface and waters in the minor groove crevice are nearly identical with those observed in the d(m^5CG) and d(CG) sequences as Z-DNA. This structure thus provides a molecular basis for the increased stability of Z-DNA in the uridine- versus thymine-containing Z-DNA sequences. The methyl groups of the thymine bases disrupt binding of a well-structured magnesium complex at the major groove surface, replacing this with a highly distorted sodium

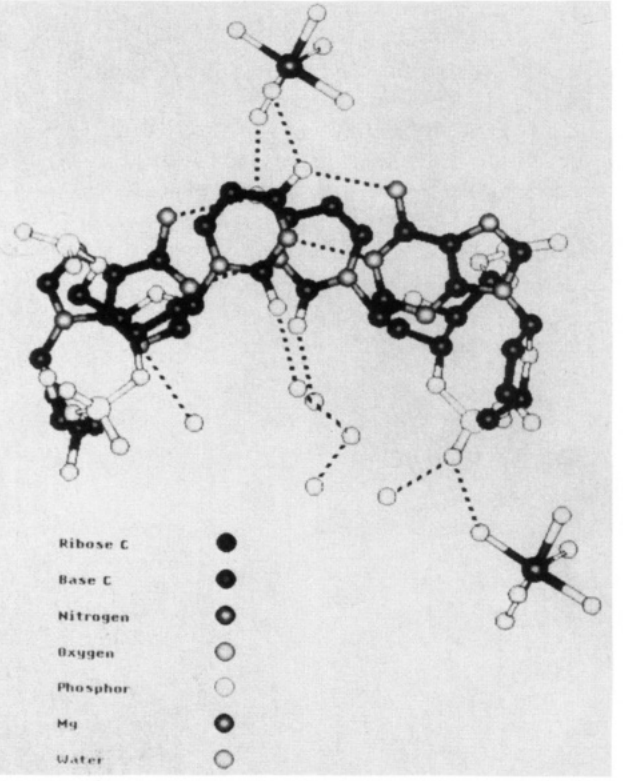

FIGURE 7: Ball and stick model showing the solvent interactions around the d(UA) dinucleotides that differ from d(TA) dinucleotides in Z-DNA. Coding of the atoms and bonds in different intensities of gray is shown in the figure key. Atoms that are within the proper distances to form hydrogen bonds are connected by broken lines. This figure shows a view of the d(UA) dinucleotides down the Z-DNA helix, along with the magnesium complex that bridges the two base pairs at the major groove surface and the waters observed in the minor groove crevice.

ion cluster. The spine of waters in the minor groove crevice is continuous in the d(UA) sequence but is disrupted in the d(TA) sequence.

Discussion

In this study, we have crystallized the self-complementary sequence d(m^5CGUAm^5CG) and found it to be left-handed Z-DNA. The equilibrium conditions required to form Z-DNA crystals of this sequence were significantly lower than those for the sequence d(m^5CGTAm^5CG) and higher than those of d(m^5CG)$_3$. This result supports our previous assertion that the methyl group at the C5 position of thymine destabilizes Z-DNA by increasing the overall hydropobicity of the major groove surface, and thus decreasing the accessibility of this surface to solvent interactions. The 1.3 Å resolution structure of d(m^5CGUAm^5CG) provides a model to test, at the molecular level, the predictions from calculations of solvent-accessible surfaces concerning the solvent interactions at the major groove surface of Z-DNA. In addition, some surprising effects to the properties of the minor groove crevice of Z-DNA were observed resulting from altering the solvent properties at the major groove surface of Z-DNA.

In this d(UA)-containing structure, we were able to locate a stucturally well-defined octahedral magnesium–water cluster bridging the O4 oxygens of uridine bases at the major groove surface of the internal d(UA) dinucleotide. The cations at the analogous surface of the d(m^5CGTAm^5CG) structure are highly distorted in terms of bond lengths and bond angles and can be more reliably assigned to either sodium complexes or water networks. Thus, the hydrophobic C5 methyls of thymine are shown to adversely disrupt solvent interactions at the major

groove of Z-DNA, as predicted by the solvent-accessible surface calculations (Kagawa et al., 1989). The surprising observation from this structure that was not predicted from comparison of the solvent-accessible surfaces of d(TA) and d(UA) dinucleotide in the Z-conformation was the effect of the methyls at the major groove surface on the structure and properties of the minor groove crevice. To the first approximation, one would expected the minor groove crevices of d(TA) and d(UA) dinucleotides in Z-DNA be nearly identical. We observed in this single-crystal structure of d(m^{5}CGUAm^{5}CG) that the minor groove crevice at the internal d(UA) dinucleotides is wider by 1.41 Å than that of the analogous dinucleotide in the d(m^{5}CGTAm^{5}CG) structure (Wang et al., 1984). This wider crevice was shown to accommodate four structurally well-defined water molecules at the internal d(UA) dinucleotides that were not observed in the minor groove crevice of the d(TA) dinucleotide of d(m^{5}CGTAm^{5}CG) (Wang et al., 1984).

The apparent absence of water in the d(TA) crevice suggests that the solvent is disordered due to thermal motion or from partial occupancy of multiple sites within the minor groove. It is likely that the Z-DNA minor groove crevice of d(TA) is too narrow to accommodate two waters per base pair but wider than necessary for binding a single water molecule. From the d(m^{5}CGUAm^{5}CG) structure, it is clear that the crevice of the d(TA) dinucleotide should have sufficient hydrogen-bonding potential to interact with two waters at each base pair, and thus, there are at least two possible sites for water interaction per base pair in the minor groove crevice. A single water molecule in the crevice may therefore be sampling multiple sites within the same d(TA) dinucleotide. Alternatively, one water may occupy one particle site within the minor groove crevice of a d(TA) base pair, while a second water occupies a different site in the crevice of a neighboring hexamer duplex within the crystal. When placed within the context of the Z-DNA crystal packing, each possible water position within the d(TA) dinucleotides minor groove is sampled and averaged over all the hexamers in the crystal. Thus, this one water molecule could appear disordered over all the hexamers in the crystal, even though it is well-defined within each d(TA) base pair.

The Z-DNA structures of d(CG)$_3$ (Wang et al., 1979), d(m^{5}CG)$_3$ (Fujii et al., 1982), and even d(CGCGTG) (Ho et al., 1985), where there are two mismatched d(TG) base pairs introduced into the structure, all show two well-structured water molecules interacting in the minor groove crevice at each base pair. These waters form a continuous hydrogen-bonded network of water molecules lining the minor groove crevice to accommodate the hydrogen-bonding potential of the DNA. The presence of two well-defined waters per base pair in the crevice of the d(UA) dinucleotides shows that the continuity of the spine of waters is maintained in the minor groove crevice of Z-DNA structures, while d(TA) disrupts this solvent spine. An analogous spine of waters has been observed in crystal structures of oligonucleotides as B-DNA (Drew & Dickerson, 1981). These continuous networks of water molecules are thought to be important for stabilizing sequences as Z-DNA or as B-DNA (Fujii et al., 1982; Wang et al., 1979; Drew & Dickerson, 1981). In the single-crystal structures of the sequences d(m^{5}CGTAm^{5}CG) (Wang et al., 1984) and d(CACGTG) (Coll et al., 1988) as Z-DNA, no structured waters were located in the minor groove at the d(TA) base pairs. This suggests that disruption of the continuous spine of waters in the Z-DNA minor groove crevice by d(TA) base pairs destabilizes the Z-DNA structure.

The disruption of the water network in the minor groove crevice and the subsequent destabilization of the Z-DNA structure by d(TA) base pairs would, at first, appear to be unrelated to the thymine methyl groups at the major groove surface. However, when we compare d(UA) and d(TA) in Z-DNA, it is clear that in fact removing these methyls from the C5 position of thymine restores the continuity of the spine of waters in the minor groove crevice. This demonstrates that a structural effect on the major groove surface can be translated through the rigid Z-DNA helix to affect the properties of the minor groove crevice, through mechanisms that are either intrinsic or extrinsic to the DNA structure. Since this is a long-range interaction, one would suspect that an electrostatic attraction between the magnesium complex at the major groove surface and the negative phosphates lining the minor groove could pull the phosphodiester toward the major groove, thus widening the minor groove crevice. The distance separating the magnesium complex from the phosphate group that is rotated in the Z-DNA structure of the d(UA) dinucleotides is 13.05 Å from the center of the magnesium to the phosphorus and 13.43 Å to the point representing the mass average of the phosphate group. When we place the d(UA) dinucleotide in the same conformation as the d(TA) dinucleotide, however, these distances are 13.03 and 13.42 Å, respectively, for the magnesium to the phosphorus and the magnesium to the center of the phosphate group. The differences between the distances separating the cation and anion are thus not great for the two conformations. If electrostatic interactions are responsible for altering the structure of the minor groove, the mechanism involved must be very subtle.

Alternatively, we can envision how demethylation of thymine could induce shearing of the adjacent base pairs that can ultimately be translated into a widening of the minor groove crevice. Demethylating a pyrimidine base effectively removes a weak electron-donating substituent group at the C5 position. Conversely, the observed substitution of monovalent sodium in the d(TA) with a divalent magnesium complex in the d(UA) structure of Z-DNA would alter the electron-withdrawing properties of the cation complex at the major groove surface. These modifications in the substituent effects would result in a redistribution of the partial charges within the aromatic bases and subsequently would alter the energy and arrangement of the stacking between the adjacent base pairs. This could shift one base pair relative to its neighbor and be observed as a shearing of the two adjacent base pairs, as seen when the d(UA) and d(TA) dinucleotides in Z-DNA are compared. The magnesium cluster at the major groove surface of the d(UA) Z-DNA structure may introduce a geometric constraint on the base stacking in addition to, or in lieu of, the electrostatic effect on the charge distribution within the bases. The cation complexes at the major groove surface of the d(TA) dinucleotide in Z-DNA are highly distorted in terms of geometry and bond distances, indicative of sodium–water complexes. The more rigid octahedral water complex of magnesium observed at the major groove surface of the d(UA) dinucleotides would necessitate some readjustment in the stacking of the adjacent base pair to accommodate the hydrogen bonds formed between the waters of the cation complex and the O_4 oxygens of the uridine bases. Thus, demethylating the thymine base may affect the stacking of the adjacent base pairs in Z-DNA either intrinsically or extrinsically.

This shearing of the adjacent base pairs in Z-DNA by demethylation of the thymine bases would be translated into concerted rotations of the ribose and phosphates that bridge the base pairs, resulting in the widening of the minor groove

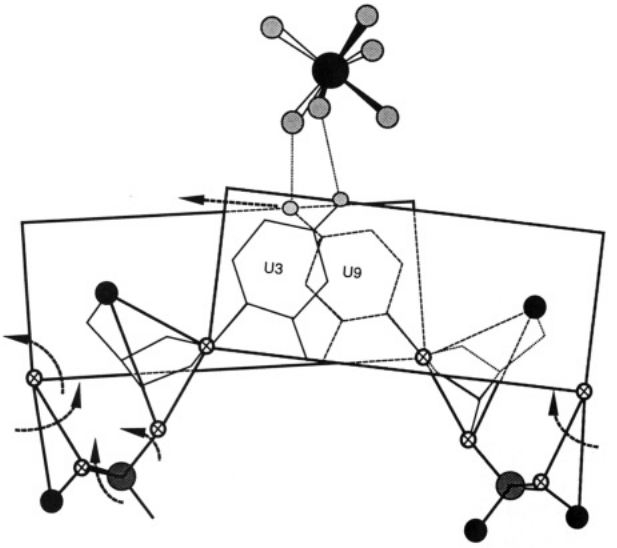

FIGURE 8: Schematic summary of the structural differences between d(UA) and d(TA) dinucleotides in Z-DNA. Planes represent the paired bases of U3-A10 and A4-U9 as viewed down the helical axis of the adjacent base pairs. The O4 oxygens of each uridine are shown as stippled atoms. Dotted lines show the hydrogen bonding between the waters of the magnesium cluster and the O4 oxygens of the uridine bases. The riboses are represented by triangles whose vertices are defined by the C1′ carbon and the O3′ and O5′ oxygens. All points of free bond rotations between structurally rigid groups are indicated by a circled ×, while points that are physically fixed by either adjacent d(m^5CG) base pairs or metal clusters are indicated by the filled circles. The straight arrow indicates the direction of the sheared base pair, while the curved arrows show the direction of rotation around points of free rotation.

crevice, as observed when the d(TA) and d(UA) dinucleotide structures of Z-DNA are compared. A simple representation of the rotational degrees of freedom for the major groups within a dinucleotide in Z-DNA is shown in Figure 8. The structural features of the DNA and the magnesium cluster are reduced to simple geometric elements, demonstrating the concerted motion of atoms within a group. The uracil–adenine base pairs are shown as rectangular planes and the riboses as triangular planes. The top rectangular plane represents base pair U3-A10, and the bottom rectangle is the A4-U9 base-pair plane. The adjacent d(UA) base-pair planes are allowed to shear relative to each other, while each ribose can rotate around points defined by the C1′ carbon and the O5′ and the O3′ oxygens. The O5′ of U3 and U9 and the O3′ of A4 and A10 vertices of each ribose are fixed by the d(m^5CG) base pairs flanking either side of the adjacent d(UA) base pairs. One of the oxygens of the phosphate bridging U9 and A10 is fixed by a magnesium cluster bound to an adjacent hexamer duplex. Within the context of these fixed geometric shapes, a minor shearing of the adjacent base planes can be seen to be accentuated through concerted rotation of the connecting riboses and phosphates to result in a significant widening of the minor groove crevice.

In conclusion, the methyl group at the C5 position of thymine bases destabilizes Z-DNA by disrupting solvent interactions, in particular the interactions of cation complexes, at the major groove surface. Removing this methyl group facilitates the binding of an octahedral cation complex at the major groove surface of Z-DNA and, subsequently, increases the accessibility of the minor groove crevice to solvent molecules. The mechanism by which structural perturbations are transmitted through the Z-DNA helix to affect the properties of the opposing helical groove is subtle and is currently being studied by substituting the magnesium complex at the d(UA) major groove surface with cation complexes that are characterized by different charges and coordination geometry constraints.

ACKNOWLEDGMENTS

We thank Dr. R. McPharland for his help in oligonucleotide synthesis, Dr. D. Keszler for his help in collecting the X-ray diffraction data, and Professor G. J. Quigley for his thoughtful discussions.

REFERENCES

Behe, M., & Felsenfeld, G. (1981) *Proc. Natl. Acad. Sci. U.S.A. 78*, 1619–1623.

Coll, M., Fita, I., Lloveras, J., Subirana, J. A., Bardella, F., Huynh-Dinh, T., & Igoleu, J. (1988) *Nucleic Acids Res. 16*, 8695–8705.

Drew, H. R., & Dickerson, R. E. (1981) *J. Mol. Biol. 151*, 535–556.

Fujii, S., Wang, A. H.-J., van der Marel, G., van Boom, J. H., & Rich, A. (1982) *Nucleic Acids Res. 10*, 7879–7892.

Hendrickson, W. A., & Konnert, J. (1979) in *Biomolecular Structure, Conformation, Function, and Evolution* (Srinivasan, R., Ed.) pp 43–57, Pergamon Press, Oxford.

Ho, P. S., Frederick, C. A., Quigley, G. J., van der Marel, G., van Boom, J. H., Wang, A. H.-J., & Rich, A. (1985) *EMBO J. 13A*, 3617–3623.

Ho, P. S., Quigley, G. J., Tilton, R. F., Jr., & Rich, A. (1988) *J. Phys. Chem. 92*, 939–945.

Jovin, T. M., McIntosh, L. P., Arndt-Jovin, D. J., Zarling, D. A., Robert-Nicoud, M., van de Sande, J. H., Jorgensen, K. F., & Eckstein, F. (1983) *J. Biomol. Struct. Dyn. 1*, 21–57.

Jovin, T. M., Soumpasis, D. M., & McIntosh, L. P. (1987) *Annu. Rev. Phys. Chem. 38*, 521–560.

Kagawa, T., Stoddard, D., Zhou, G., & Ho, P. S. (1989) *Biochemistry 28*, 6642–6651.

Kollman, P., Weiner, P., Quigley, G. J., & Wang, A. (1982) *Biopolymers 21*, 1945–1969.

Rich, A., Nordheim, A., & Wang, A. H.-J. (1984) *Annu. Rev. Biochem. 53*, 791–846.

Wang, A. H.-J., Hakoshima, T., van der Marel, G., van Boom, J. H., & Rich, A. (1984) *Cell 37*, 321–331.

Wang, A. H.-J., Quigley, G. J., Kolpak, F. J., Crawford, J. L., van Boom, J. H., van der Marel, G., & Rich, A. (1979) *Nature (London) 282*, 680–686.

Wang, A. H.-J., Quigley, G. J., Kopak, F. J., van der Marel, G. A., van Boom, J. H., & Rich, A. (1981) *Science 211*, 171–176.